biomolecules

MDPI

céArticle

Isoprostanoid profiling of marine microalgae

Claire Vigor [1]*, Camille Oger [1], Guillaume Reversat [1], Amandine Rocher [1], Bingqing Zhou [1], Amandyne Linares-Maurizi [1], Alexandre Guy [1], Valérie Bultel-Poncé [1], Jean-Marie Galano [1], Joseph Vercauteren [1], Thierry Durand [1], Philippe Potin [2], Thierry Tonon [2,3] and Catherine Leblanc [2]

[1] Institut des Biomolécules Max Mousseron, IBMM, Université de Montpellier, CNRS, ENSCM, Faculté de Pharmacie, 34093 Cedex 5 Montpellier, France ; claire.vigor@umontpellier.fr

[2] Integrative Biology of Marine Models, LBI2M (Sorbonne Université/CNRS), Station Biologique de Roscoff (SBR), 29680 Roscoff, France ; catherine.leblanc@sb-roscoff.fr

[3] Centre for Novel Agricultural Products, Department of Biology, University of York, Heslington, York, YO10 5DD, United Kingdom; thierry.tonon@york.ac.uk

* Correspondence: claire.vigor@umontpellier.fr ; Tel.: +33411957513

Received: date; Accepted: date; Published: date

Abstract: Algae result from a complex evolutionary history that shapes their metabolic network. For example, these organisms can synthesize different polyunsaturated fatty acids, as those found in land plants and oily fish. Due to the presence of numerous double bonds, such molecules can be oxidized non-enzymatically, and this results in the biosynthesis of high-value bioactive metabolites named isoprostanoids. So far, there have been only a few studies reporting isoprostanoids production in algae. To fill this gap, the current investigation aimed at profiling isoprostanoids by LC-MS/MS in four marine microalgae. A good correlation was observed between the most abundant PUFAs produced by the investigated microalgal species and their isoprostanoid profiles. No significant variations in the content of oxidized derivatives were observed for *Rhodomonas salina* and *Chaetoceros gracilis* under copper stress, whereas increases in the production of C18-, C20- and C22-derived isoprostanoids were monitored in *Tisochrysis lutea* and *Phaeodactylum tricornutum*. In the presence of hydrogen peroxide, no significant changes were observed for *C. gracilis* and for *T. lutea*, while variations were monitored for the other two algae. This study paves the way to further studying the physiological roles of isoprostanoids in marine microalgae, and exploring these organisms as bioresources for isoprostanoid production.

Keywords: microalgae, PUFAs, isoprostanoids, oxidative stress, micro-LC-MS/MS

1. Introduction

Marine ecosystems account for approximately half of the global primary production, and unicellular eukaryotes, e.g. photosynthetic microalgae, as part of the phytoplankton, are major contributors to this ocean productivity [1]. These organisms also play critical roles in biogeochemical cycle of many chemical elements including carbon, nitrogen, sulfur, phosphorus and silica. Currently, more than 35,000 species of microalgae have been described, which likely represent only a small part of the supposed biodiversity since their number of species has been estimated to range between 200,000 and 800,000 [2].

Microalgae can grow mostly autotrophically, but also heterotrophically, or mixothrophically according to culture conditions and metabolic capacities. These are related to the different environments inhabited by these organisms, as well as their evolutionary history which shaped their

network of biochemical pathways [3]. Some microalgae exhibit high contents in proteins, lipids, sugars and pigments, making them attractive for a number of biotechnological applications. Such potential has been investigated for the bio-based production of a wide range of compounds for the food, feed, energy, agriculture and health sectors [4].

Among the interesting compounds produced by microalgae are the omega-3 (ω-3 or n-3) long-chain polyunsaturated fatty acids (n-3 PUFAs), eicosapentaenoic acid (EPA; C20:5n-3), and docosahexaenoic acid (DHA; C22:6n-3). While land plants and microalgae can produce the medium chain α-linolenic acid (ALA; C18:3n-3), only the latter organisms can convert this precursor into EPA and DHA. These three fatty acids are considered as essential in human nutrition because ALA cannot be synthesized de novo by humans, and the metabolic conversion efficiency of dietary ALA into EPA and DHA is low and insufficient to meet physiological demands [5]. These n-3 PUFAs have been shown to provide significant benefits on human health [6, 7], notably in mitigating a number of pathological conditions including cardiac diseases [8]. They are also important for healthy development of the neural system [9, 10], and as such they are necessarily included in infant formula. Very recently, it has been proposed that dietary n-3 PUFAs selectively drive expansion of adipocyte numbers to produce new fat cells and store saturated fatty acids, enabling homeostasis of healthy fat tissue [11]. At present, marine fishes and fish oils are the main commercial sources of n-3 PUFAs. However, the suitability of these sources of PUFAs for human consumption has been questioned, notably because of biosafety (e.g. content in heavy metals), and of overfishing. In addition, the current supply of n-3 PUFAs from these traditional sources is insufficient to satisfy human nutritional requirements [12]. Therefore, new sources of n-3 PUFAs have been investigated, such as wild type and engineered microbes including microalgae [13], and extraction of fish oil from genetically modified crops [14].

It is well established that PUFAs are highly reactive species sensitive to oxidation because of the presence of bis-allylic structures in which α-hydrogen atoms are easily removed by action of free radicals. Some of these free radicals, named reactive oxygen species, are produced under oxidative stress (OS) conditions, and react with PUFAs to form, spontaneously through enzymatic reactions, oxidized derivatives of PUFAs. All of these oxidized metabolites are grouped under the term oxylipins. Most of the oxylipins studied so far are derived from enzymatic transformation catalyzed by enzymes such as lipoxygenases or dioxygenases. During the last two decades, it has been shown that non-enzymatic oxidation of PUFAs (NEO-PUFAs) leads to other valuable compounds. ALA are precursors of phytoprostanes (PhytoPs), arachidonic acid (AA; C20:4n-6) of isoprostanes from the serie 2 (IsoPs, serie 2), EPA of isoprostanes from the serie 3 (IsoPs, serie 3), AdA (docosatetraenoic acid; C22:4n-6) of dihomo-isoprostanes and dihomo-isofurans, and DPA_{n-6} (docosapentaenoic acid; C22:5n-6) and DHA of neuroprostanes (NeuroPs) (Figure 1 and Figure 2). These NEO-PUFAs are considered to be very good markers of OS in plants and animals. They have also been shown to act as lipid mediators with key functions in various cell signaling pathways [15], and have been suggested to be potentially beneficial for human health [16].

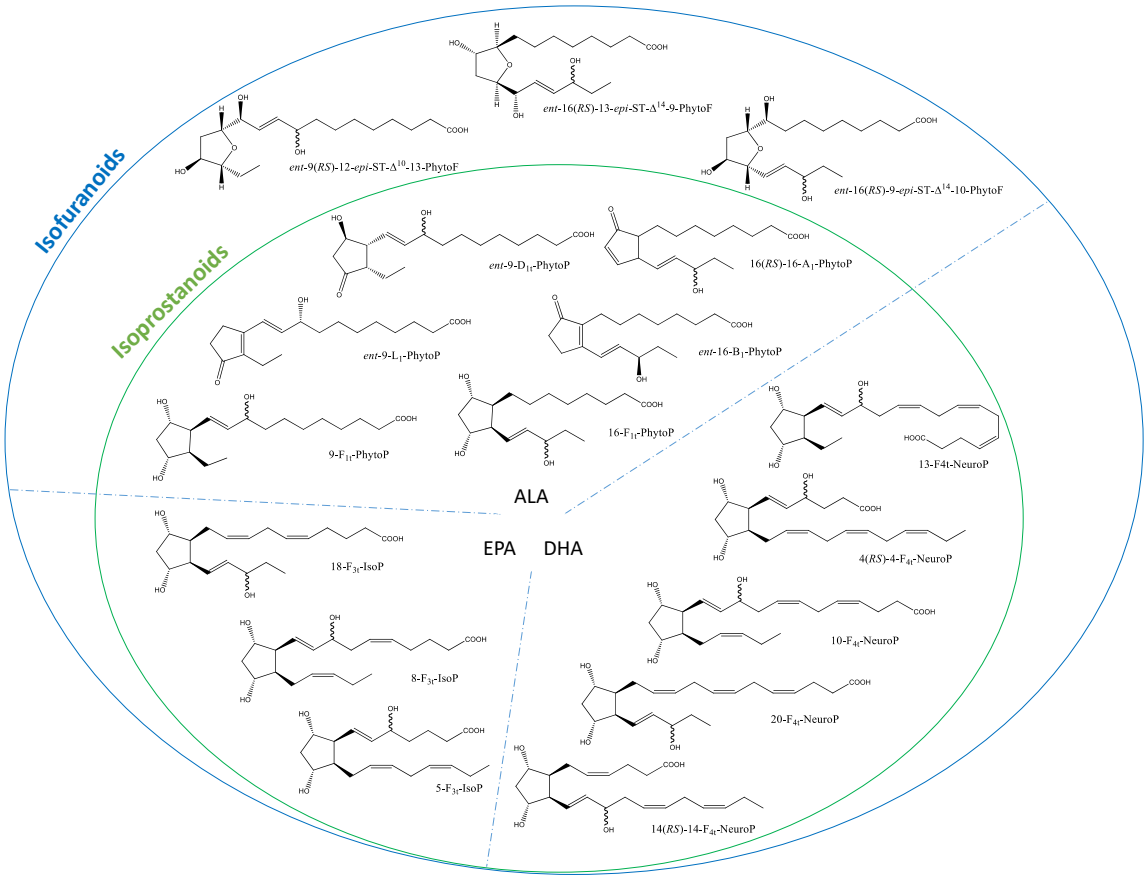

Figure 1. : Structure of some isoprostanoids isomers derived from n-3 PUFAs : ALA (α-linolenic acid), EPA (eicosapentaenoic acid) and DHA (docosahexaenoic acid)

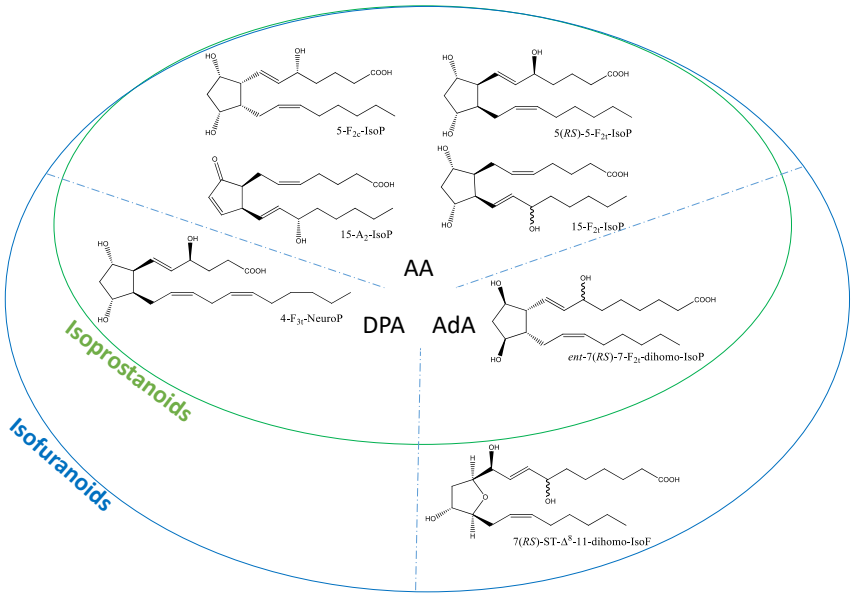

Figure 2. : Structure of some isoprostanoids isomers derived from n-6 PUFAs : AA (arachidonic acid), DPA n-6 (docosapentaenoic acid) and AdA (adrenic acid)

Recently [17], we have investigated variations in isoprostanoid content of red and brown macroalgae after exposure to oxidative (heavy metal) stress condition [18]. In addition, changes in production of isoprostanoids derived from C18, C20, and C22 fatty acids were observed in the

microalga *Phaeodatylum tricornutum* subjected to oxidative stress by cultivation under increasing doses of hydrogen peroxide (H_2O_2) [19]. This work suggested that non-enzymatic oxylipins in *P. tricornutum* may be involved in the control of important processes under various physiological and environmental conditions. In view of these findings, and to go further in the study of potential production of NEO-PUFAs by algae, we were first interested in increasing knowledge on the distribution of NEO-PUFAs in different lineages of marine microalgae by establishing qualitative and quantitative profiles under laboratory culture growth conditions. Based on previous analysis of fatty acids and lipid composition in marine microalgae, and notably the high production of EPA and DHA by some of them [20-22], we decided to select the four following species : the diatoms *Phaeodactylum tricornutum* and *Chaetoceros gracilis* known to exhibit high content of EPA, the haptophyte *Tisochrysis lutea* that has been shown to produce elevated amounts of ALA and DHA, and the cryptophyte *Rhodomonas salina* that harbor similar and high levels of EPA and DHA. Our second objective was to assess changes in the isoprostanoid profiles of the selected microalgae under altered physiological conditions, in relationships with the exposure to oxidative stress (copper and hydrogen peroxide treatments).

2. Materials and Methods

2.1. Chemicals and reagents

All the NEO-PUFA analytical standards, as well as the internal standard mixture (C19-16-F_{1t}-PhytoP and C21-15-F_{2t}-IsoP) used to determine the calibration curve ratio, were synthesized according to previously described procedures [23-26]. NEO-PUFA analytical standards were as follow: phytoprostanes (9-L_1-PhytoP, *ent*-9-L_1-PhytoP, *ent*-16-*epi*-16-F_{1t}-PhytoP, 9-F_{1t}-PhytoP, 16-F_{1t}-PhytoP + 9-*epi*-9-F_{1t}-PhytoP, 16(*RS*)-16-A_1-PhytoP, 16-B_1-PhytoP, and *ent*-16-B_1-PhytoP), phytofurans (*ent*-16(*RS*)-9-*epi*-ST-Δ^{14}-10-PhytoF, *ent*-9(*RS*)-12-*epi*-ST-Δ^{10}-13-PhytoF, *ent*-16(*RS*)-13-*epi*-ST-Δ^{14}-9-PhytoF) coming from oxidation of the C18 n-3 ALA, isoprostanes derived from the C20 n-6 AA (15-F_{2t}-IsoP, 15-*epi*-15-F_{2t}-IsoP, 5-F_{2t}-IsoP and 5-*epi*-5-F_{2t}-IsoP, 5-F_{2c}-IsoP), isoprostanes coming from the oxidation of C20 n-3 EPA (8-F_{3t}-IsoP, 8-*epi*-8-F_{3t}-IsoP, 18-F_{3t}-IsoP, 18-*epi*-18-F_{3t}-IsoP), dihomo-isoprostanes and dihomo-isofurans derived from the C22 n-6 AdA (*ent*-7(*RS*)-7-F_{2t}-dihomo-IsoP, 7(*RS*)-ST-Δ^8-11-dihomo-IsoF), neuroprostanes coming from the oxidation of C22 n-3 DHA (4(*RS*)-4-F_{4t}-NeuroP, 10-F_{4t}-NeuroP, and 10-*epi*-10-F_{4t}-NeuroP, 20-F_{4t}-NeuroP et 20-*epi*-20-F_{4t}-NeuroP), and those derived from the oxidation of C22 DPA_{n-6} (4(*RS*)-4-F_{3t}-$NeuroP_{DPAn-6}$). The only exception is 16 (*RS*)-16-A_1-PhytoP that was purchased from Cayman Chemicals (Ann Arbor, MI, USA). LC-MS grade water, methanol, acetonitrile and chloroform were obtained from Fisher Scientific (Loughborough, UK). Hexane (CHROMASOLV for HPLC), formic and acetic acid, ammonia, and potassium hydroxide (Fluka for mass spectrometry) were purchased from Sigma-Aldrich (Saint Quentin Fallavier, France). Ethyl acetate (HPLC grade) was acquired from VWR (EC). Solid phase extraction (SPE) cartridges Oasis MAX with mixed polymer phase (3 mL, 60 mg) were obtained from Waters (Milford, MA, USA).

2.2. Microalgal species

The four microalgae (*Tisochrysis lutea* RCC 1349, *Phaeodactylum tricornutum* RCC 69, *Chaetoceros gracilis* and *Rhodomona salina* RCC 20) used in this study were obtained from the Roscoff Culture Collection (RCC) and from the EMBRC Roscoff culture facilities for *C. gracilis*. This latter strain is a kind gift from the Experimental Mollusc Hatchery of Ifremer at Argenton (France) and is cultivated for larvae feeding (Robert et al. 2004, https://archimer.ifremer.fr/doc/2004/rapport-1546.pdf).

135

136 *2.3. Cultivation of microalgae and oxidative stress treatments*

137 Microalgae were grown in Conway medium [27], commonly used in aquaculture, at a
138 temperature of 18° C and under continuous light intensity of 300 µmoles m^{-2} s^{-1} for biomass
139 production [28, 29]. The volume of culture was gradually brought, by successive subculture in
140 increasing volumes of medium, to a final volume of 10 L in Nalgene flasks placed under constant
141 aeration. Cells were harvested after reaching the stationary phase. After centrifugation (5,000 rpm for
142 25 min), the supernatant was removed, and the pellet resuspended in 2 L of 0.45 µm filtered and
143 autoclaved natural seawater (FSW) collected offshore at Roscoff (at a site with no direct chemical
144 influence from the shore), and free of organic matter. After agitation to ease resuspension, cells were
145 spun down again for 25 minutes at 5,000 rpm, then resuspended as described above in a final volume
146 of 900 ml. This suspension was split into nine glass flasks previously washed overnight with 1% HCl
147 to limit Cu adsorption and rinsed with mqH_20 and FSW. The 100 ml cell volume was brought to 1 L
148 with FSW. Three flasks were considered as control, three were used for copper stress (Cu(II) as
149 $CuCl_2$), and three for incubation in presence of hydrogen peroxide (H_2O_2).
150 Oxidative stress was triggered by adding Cu(II) as $CuCl_2$ (Merck, Germany) at a final
151 concentration of 0.3 µM, or H_2O_2 at 1 mM. After 24 h of incubation under conditions described above,
152 cells were harvested as explained in the previous section. Supernatants were discarded, and cells
153 were washed one time using FWS and centrifugated, before freezing in liquid nitrogen and freeze-
154 drying. Algal material was stored at -20°C until analysis.

155 *2.4. Preparation of algal samples for lipidomic analysis*

156 During the preparation of samples for such analysis, we made two important observations. First,
157 we noticed that one sample of *P. tricornutum* obtained under H_2O_2 stress condition contained some
158 water after lyophylization. This sample was not considered further for extraction. In addition, one
159 sample of *T. lutea* obtained after copper stress shown significant difference in color and texture during
160 the extractive process when compared to the other samples. The data acquired in LC-MS/MS for this
161 latter sample showed numerous outliers (Grubbs's statistical test; data not shown), which were
162 discarded for subsequent analysis.
163 A protocol similar to what was described for our previous work on macroalgae was applied for
164 lipidomic analysis [18]. Freeze-dried microalgal samples were coarsely reduced to powder using first
165 a Mixer Mill MM400 (Retsch®) bench top unit. Then 100 mg of powder were added in grinding matrix
166 tubes (Lysing matrix D, MP Biochemicals, Illkirch, France) with 25 µL of BHT (Butylated
167 hydroxytoluene 1% in water) and 1 mL of MeOH. Tubes were placed in a FastPrep-24 (MP
168 Biochemicals), and samples were ground for 30 s at a speed of 6.5 m/s. Suspensions were transferred
169 into 15-ml centrifuge tube, and 1 mL of MeOH, 4 µL of IS (1 ng/µL), and 1.5 mL of phosphate buffer
170 (50 mM pH 2.1, prepared with NaH_2PO_4 and H_3PO_4) saturated in NaCl were added. Tubes were then
171 stirred for 1 hour at 20 °C. Subsequently, the mixture was vortexed and centrifuged at 5,000 rpm for
172 5 min at room temperature. The organic phase was recovered in Pyrex tubes, and the solvent was
173 dried under a stream of nitrogen at 40 °C. Afterward, lipids were hydrolyzed with 950 µL of KOH
174 for 30 min at 40 °C. After incubation, 1 mL of formic acid (FA; 40 mM, pH 4.6) was added before
175 running the SPE separation. First, SPE Oasis MAX cartridges were conditioned with 2 mL of MeOH
176 and equilibrated with 2 mL of formic acid (20 mM, pH 4.5). After loading the sample, the cartridges
177 were successively washed with: 2 mL of NH_3 (2 % (v/v)), 2 mL of a mixture of formic acid (20 mM):
178 MeOH (70:30, v/v), 2 mL of hexane, and finally 2 mL of a hexane: ethanol: acetic acid (70:29.4:0.6,
179 v/v/v) mixture. Lastly, all samples were evaporated to dryness under a nitrogen flow at 40 °C for 30

min, and reconstituted in 100 µL of mobile phase (solvent A: water with 0.1% (v/v) of formic acid; solvent B: ACN/MeOH; 8:2, v/v; with 0.1% (v/v) of formic acid; A/B ratio, 83:17) for injection.

2.5. Preparation of samples for analysis of extraction yield and matrix effect

Parameters related to extraction yield (EY) and matrix effect (ME) were determined for a better description of microalgal isoprostanoid profiles. To this aim, three sets of samples were prepared. The first one was obtained by addition of 6.4 µL of two different concentrations of a standard mixture (36 PUFAs oxidized metabolites at 0.5 and 8 ng/mL) into 100 mg of freeze-dried microalgae at the beginning of the extraction process described above to reach a concentration of 32 and 512 ng/g respectively. This corresponds to the "pre-spiked samples". For the second set of samples, extraction was done as explained in the previous section on 100 mg of microalgae up to the elution step. Then, eluates were spiked with 6.4 µL of the two different concentrations of standard mixture used for the "pre-spiked samples", and processed to complete the algal sample preparation protocol. These samples were named "post-spiked samples". The third set of samples consisted of standard solutions (final concentrations of 32 and 256 ng/mL) prepared in 100 µL of mobile phase H_2O/ACN/FA (83:17:0.1; v/v/v). All sets of samples were analyzed using the LC-MS/MS system described below. The EY was calculated as the percentage difference between peaks areas of standards in pre-spiked and post-spiked samples. The ME was determined as the percentage difference between peak areas of standard added to the extracted samples (post-spiked sample) and pure standards diluted into mobile phase. The ME and EY were calculated for each isoprostanoid and for each species.

2.6. Micro-LC-MS/MS analysis

All LC-MS analyses were carried out using an Eksigent® MicroLC 200 plus (Eksigent Technologies, CA, USA) on a HALO C18 analytical column (100 * 0.5 mm, 2.7 µm; Eksigent Technologies, CA, USA) kept at 40°C. The mobile phase consisted of a binary gradient of solvent A (water with 0.1% (v/v) of formic acid) and solvent B (ACN/MeOH; 8:2, v/v; with 0.1% (v/v) of formic acid). The elution was performed at a flow rate of 0.03 mL/min using the following gradient profile (min/%B): 0/17; 1.6/17; 2.85/21; 7.3/25; 8.8/28.5; 11/33.3; 15/40; 16.5/95; 18.9/95, and then returned to the initial conditions. Under these conditions, no sample contamination or sample-to-sample carry-over was observed.

Mass spectrometry analyses were performed on an AB SCIEX QTRAP 5500 (Sciex Applied Biosystems, ON, Canada). The ionization source was electrospray (ESI), and it was operated in the negative mode. The source voltage was kept at −4.5 kV, and N_2 was used as curtain gas. The multiple ion monitoring (MRM) of each compound were predetermined by MS/MS analysis to define the two transitions for quantification (T_1) and specification (T_2) (Table S1). The analysis was conducted by monitoring precursor ion to product ion (T_1). Peak detection, integration and quantitative analysis were performed by MultiQuant 3.0 software (Sciex Applied Biosystems). The quantification of isoprostanoids was based on calibration curves obtained from the analyte to IS area under the curve ratio. Linear regression of six concentrations of standards mixture (16, 32, 64, 128, 256 and 512 pg/µL) of each standard were calculated. The sensitivity of the method was evaluated through limit of detection (LOD) and limit of quantification (LOQ) parameters which were defined as the lowest concentration with a signal to noise ratio above 3 and 10 respectively.

2.7. Statistical analysis

All statiscal analysis was perform with R ~~[28]~~[30], all graphics were created with differents functions of the tidyverse package ~~[29]~~[31] and all the tables with kableExtra package ~~[30].~~[32]. Analyte concentrations were compared by one-way analysis of variance (ANOVA) and post-hoc (Tukey) test for multiple comparison using rstatix package ~~[31].~~[33]. For all analyses, the significance threshold was 0.05 for the p value resulting from the statistical test used.

3. Results

3.1. Analysis of extraction yield and matrix effect

The analysis of NEO-PUFAs in natural matrices is extremely challenging, requiring highly sensitive and specific methods for their profiling and characterization. Therefore, a protocol relying on specific extraction of lipophilic compounds (Folch extraction), combined with a step of SPE to eliminate potentially interfering substances, was implemented to obtain an extract enriched in NEO-PUFAs. Such protocol has proven to be efficient for similar analysis in the past [~~32, 33~~34, 35]. Isoprostanoids were subsequently separated, identified, and quantified using a micro-LC-MS/MS method validated by previous studies [~~34-~~36-38]. Identification relied on retention times observed during spiked experiments, determination of molecular masses, and analysis of specific MS/MS transitions. Calibration curves for the calculation of the concentrations were established for 32 compounds (Table S2), as well as LODs and LOQs. Values were found to be dependent of the type of isoprostanoids, and ranged between 0.16 and 0.63 pg injected for LODs, and between 0.16 and 1.25 pg injected for LOQs. In addition, based on previous experiments done on macroalgae (Vigor et al. 2018), we decided to assess the influence of matrix effect (ME) on the extraction protocol since this can affect extraction yields (EY) and/or mass ionization. Therefore, algal samples spiked with two different concentrations of a standard mixture (SM_{32} or SM_{256}) were analyzed to calculate of the EY and the ME, which subsequently enable determination of the efficiency of the sample processing (Table S3). The extraction yield, a parameter specific to each compound (standards and IS), allowed the evaluation of product losses that could happen by retention on the SPE cartridge and/or by partial elution during the washing steps. For the majority of analytes of *C. gracilis* and *R. salina*, the apparent loss of compounds during SPE was between 10% and 20%. The results were most often similar for the two spiked concentrations (32 and 512 ng/g). Regarding the type of compounds (PhytoPs, PhytoFs, IsoPs or NeuroPs), no specific trend was noticed. As far as *P. tricornutum* and *T. lutea*, the calculated extraction yield was more than 100% for some analytes, corresponding probably to the co-elution of a compound that presents the same MRM transition. Note in the table the values of two or even three units considered to be outliers. To complete this validation, the matrix effect, corresponding to an ion-suppression/enhancement of co-eluted matrix compounds, was evaluated. As for EY, ME is specific to each isoprostanoid, and there was no similar behavior across the same class of compounds, neither across selected species.

For the sake of clarity, results are presented species by species in the next sections. In addition, Table 1 provides a summary of the relative percentage distribution of each type of isoprostanoid (ALA, AA, EPA; AdA, EPA, DPA, DHA) in the four species studied.

Table 1: Relative percentage distribution of each type of NEO-PUFAs in *C. gracilis, P. tricornutum, T. lutea, and R. salina.*

Microalgal species	Metabolites of ALA	Metabolites of AA	Metabolites of AdA	Metabolites of EPA	Metabolites of DPA	Metabolites of DHA
Chaetoceros gracilis						
CTL	0,8%	6,6%	0,4%	89,0%	0,0%	3,1%
Cu^{2+}	1,1%	7,4%	0,5%	87,9%	0,0%	3,0%
H_2O_2	0,8%	11,2%	0,4%	83,4%	0,0%	4,2%
Phaeodactylum tricornutum						
CTL	65,5%	4,0%	1,7%	28,2%	0,0%	0,6%
Cu^{2+}	58,1%	4,5%	2,0%	34,8%	0,0%	0,5%
H_2O_2	44,8%	4,3%	1,5%	48,7%	0,0%	0,7%
Tisochrysis lutea						
CTL	69,5%	0,2%	0,6%	0,1%	1,9%	27,7%
Cu^{2+}	73,6%	0,3%	0,8%	0,1%	2,2%	23,0%
H_2O_2	67,9%	0,2%	0,7%	0,1%	1,7%	29,4%
Rhodomonas salina						
CTL	71,2%	2,4%	0,5%	18,2%	0,1%	7,4%
Cu^{2+}	66,7%	2,7%	0,4%	21,4%	0,2%	8,6%
H_2O_2	79,1%	3,5%	1,5%	12,4%	0,1%	3,4%

3.2. *Rhodomonas salina*

Analysis of the isoprostanoid profile of this species revealed the presence of 35 isoprostanoids (Table 2) (Figure S1). The concentrations of metabolites were comprised between 13.4 ng/g for the epimers 4(*RS*)-4-F_{3t}-NeuroP and 2 µg/g for 16-B_1-PhytoP. The total amount of isoprostanoids in *R. salina* was 10.6 µg/g.

Table 2. : Quantification of NEO-PUFAs in *R. salina* incubated under control, copper or H_2O_2 stress condition. Data are mean ± Sd (n=3) expressed as ng/g dry weight. NaN stands for Not a Number because impossible value.

	CTL		Cu^{2+}		H_2O_2	
	Conc.	Sd	Conc.	Sd	Conc.	Sd
10-*epi*-10-F_{4t}-NeuroP	4.96e+01	1.81e+01	8.12e+01	5.15e+01	1.32e+01	5.03e+00
10-F_{4t}-NeuroP	4e+01	1.19e+01	6.25e+01	3.43e+01	1.51e+01	5.99e+00
13-*epi*-13-F_{4t}-NeuroP	1.13e+02	3.57e+01	1.6e+02	7.68e+01	3.92e+01	1.34e+01
13-F_{4t}-NeuroP	1.83e+02	6.52e+01	2.79e+02	1.53e+02	4.1e+01	NaN
14 (*RS*)-14-F_{4t}-NeuroP	5.1e+01	1.48e+01	8.9e+01	5.5e+01	1.23e+01	4.78e+00
15-*epi*-15-F_{2t}-IsoP	2.6e+01	7.17e+00	3.71e+01	1.54e+01	3.17e+01	9.39e+00
15-F_{2t}-IsoP	1.4e+01	3.78e+00	2.19e+01	1.01e+01	1.73e+01	6.42e+00
16-B_1-PhytoP	1.96e+03	9.69e+01	2.19e+03	2.08e+02	1.41e+03	8.44e+02
18-F_{3t}-IsoP	7.11e+02	2.39e+02	1.1e+03	5.75e+02	3.43e+02	1.42e+02
18-*epi*-18-F_{3t}-IsoP	2.4e+02	6.36e+01	3.93e+02	2.03e+02	1.74e+02	5.49e+01
20-*epi*-20-F_{4t}-NeuroP	6.7e+01	1.97e+01	9.72e+01	4.8e+01	3.73e+01	1.62e+01
20-F_{4t}-NeuroP	8.88e+01	2.87e+01	1.43e+02	8.16e+01	3.31e+01	1.14e+01
4 (*RS*)-4-F_{3t}-NeuroP	1.34e+01	4.57e+00	2.27e+01	1.68e+01	9.24e+00	1.9e+00
4 (*RS*)-4-F_{4t}-NeuroP	1.94e+02	4.5e+01	3.26e+02	1.87e+02	9.01e+01	9.4e+00
5-*epi*-5-F_{3t}-IsoP	4.57e+02	1.37e+02	7.17e+02	3.78e+02	2.78e+02	7.71e+01
5 (*RS*)-5-F_{2t}-IsoP	7.01e+01	1.77e+01	1.07e+02	4.9e+01	9.57e+01	2.23e+01
5-F_{3t}-IsoP	4.24e+02	1.07e+02	7.13e+02	3.77e+02	1.93e+02	4.33e+01
5-F_{2c}-IsoP	1.49e+02	3.1e+01	2.22e+02	9.62e+01	1.43e+02	3.49e+01
7 (*RS*)-ST-Δ^{18}-11-dihomo-IsoF	5.71e+01	3.55e+00	6.29e+01	3.56e+00	1.25e+02	2.24e+01
8-*epi*-8-F_{3t}-IsoP	3.89e+01	1.15e+01	6.14e+01	3.3e+01	1.89e+01	7.81e+00
8-F_{3t}-IsoP	5.73e+01	1.7e+01	8.2e+01	4.02e+01	1.7e+01	4.21e+00
9-*epi*-9-F_{1t}-PhytoP	5.14e+02	1.15e+02	8.51e+02	4.55e+02	6.68e+02	1.19e+02
9-F_{1t}-PhytoP	5.84e+02	1.13e+02	8.88e+02	4.04e+02	6.87e+02	1.22e+02
9-L_1-PhytoP	1.51e+03	7.66e+01	1.66e+03	1.72e+02	1.11e+03	6.19e+02
ent-16-*epi*-16-F_{1t}-PhytoP	4.4e+02	9.67e+01	7.15e+02	3.62e+02	5.5e+02	1.18e+02
ent-16-F_{1t}-PhytoP	3.11e+02	6.64e+01	5.2e+02	2.84e+02	4.17e+02	8.13e+01
ent-16(*RS*)-9-*epi*-ST-Δ^{14}-10-PhytoF	1.79e+03	1.73e+02	2.18e+03	4.11e+02	1.29e+03	NaN
ent-9(*RS*)-12-*epi*-ST-Δ^{10}-13-PhytoF	4.34e+02	NaN	5.7e+02	1.24e+02	4.04e+02	1.49e+02

Considering the four PhytoPs corresponding to epimers 9-F_{1t}-PhytoP, 9-*epi*-9-F_{1t}-PhytoP, 16-F_{1t}-PhytoP, and 16-*epi*-16-F_{1t}-PhytoP, plus two other derivatives (16-B_1-PhytoP, 9-L_1-PhytoP), and two pairs of phytofuranoid form (*ent*-16(*RS*)-9-*epi*-ST-Δ^{14}-10-PhytoF and *ent*-9(*RS*)-12-*epi*-ST-Δ^{10}-13-PhytoF), ALA is considered as the main source of isoprostanoids in *R. salina*. This is confirmed when

assessing the amounts of oxidized derivatives produced for each potential precursor. Those from ALA represent an average value of 7.6 µg/g of algal dry weight, with the 16-B_1-PhytoP and the *ent*-16(*RS*)-9-*epi*-ST-Δ^{14}-10-PhytoF being the most abundant (2 µg/g and 1.8 µg/g respectively). DHA was also inferred to produce a wide range of compounds with up to ten stereoisomeric NeuroPs that could be arranged by pairs. The sum of DHA derivatives was 0.8 µg/g, i.e. approximately ten times less than the sum of the ALA derivatives. *R. salina* also synthesized six EPA derivatives, again as epimers that can be classified by pairs, which correspond to an amount of 1.9 µg/g. Therefore, compared to DHA derived isoprostanoids, EPA products have slightly less structural diversity, but accumulated at a higher content. Among the other molecular species of interest, it is worth mentioning those derived from AA: five representatives (15-*epi*-15-F_{2t}-IsoP, 15-F_{2t}-IsoP, 5(*RS*)-5-F_{2t}-IsoP, 5-F_{2c}-IsoP) were identified, for a total content of 0.26 µg/g. To complete this description, other isoprostanoids were observed, including AdA derivatives (7(*RS*)-ST- Δ^8-11-dihomo-IsoF at the level of 0.06 µg/g), and DPA_{n-6} derivatives (4(*RS*)-4-F_{3t}-$NeuroP_{DPAn-6}$ at the level of 0.01 µg/g). Based on this analysis, it is interesting to note that, while the cryptophyte *R. salina* is known to produce high amounts of EPA and DHA [~~37~~ 39-41], the most abundant isoprostanoids were derived from the C18 ALA (71.5 % of the total amount of PUFA oxidized derivatives).

After oxidative stress, no modification in the diversity of the molecules identified could be noticed. All the compounds observed under the control condition were still present under OS condition, regardless of the type of stress applied. Few significant changes were observed in the content of the 35 NEO-PUFAs measured initially. In fact, based on statistical analysis, the amount of only one compound showed a significant increase (Tables S4) between control condition and H_2O_2 stress. Indeed, it was observed that the content of the two 7(*RS*)-ST-Δ^8-11-dihomo-IsoF epimers doubled, from 0.06 µg/g to 0.13 µg/g, after OS (Table 1). In addition, when comparing profiles obtained after copper- and peroxide hydrogen additions, differences were noted for three compounds: 8-F_{3t}-IsoP, *ent*-16(*RS*)-9-*epi*-ST-Δ^{14}-10-PhytoF, and 7(*RS*)-ST-Δ^8-11-dihomo-IsoF (Figure 3).

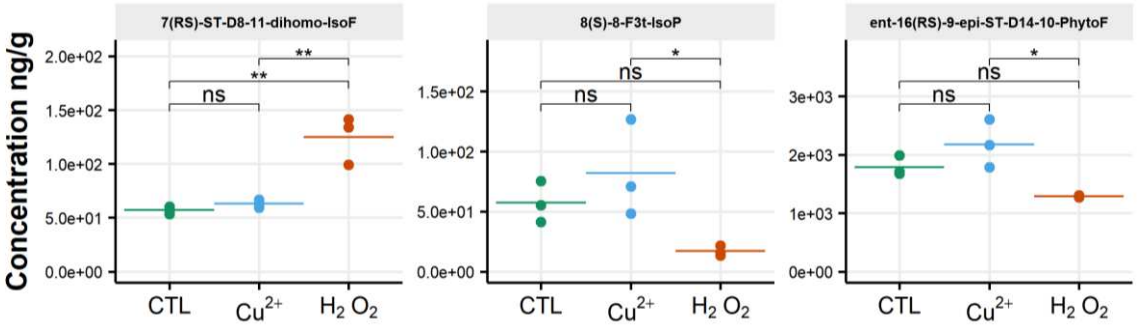

Figure 3. : Changes in content of selected isoprostanoids for the cryptophyte *R. salina* between control condition (CTL) and oxidative stress (Cu^{2+} and H_2O_2) conditions. Statistically relevant responses between control and stress conditions (one-way ANOVA) are indicated by asterisks: *, $p < 5 \times 10^{-2}$; **, $p < 5 \times 10^{-3}$; ns, not significant.

3.3. *Tisochrysis lutea*

T. lutea has a greater diversity of compounds identified compared to the other species investigated, with 38 isoprostanoids observed. This consisted in 16 derivatives coming from ALA oxidation, ten derivatives from DHA, three from EPA, three from AA, four from AdA, and finally two from DPA_{n-6}. Despite this increased diversity, the total amount of isoprostanoids measured in this haptophyte was lower than what was measured in the cryptophyte *R. salina*, i.e. 7 µg/g. The

details of the oxidized PUFAs derivatives grouped by family are as follow: 4.8 µg/g from ALA, 1.9 µg/g from DHA, 0.008 µg/g from EPA, 0.012 µg/g from AA, 0.045 µg/g from AdA, and 0.135 µg/g from $DPA_{n\text{-}6}$. The levels of individual metabolites were comprised between 1.24 ng/g for 8-*epi*-8-F_{3t}-IsoP and 0.988 µg/g for 16-B_1-PhytoP, which represents a 1000-fold difference, and indicated that isoprostanoids can be produced at very different ranges in this microalga species (Table 3).

Table 3. : Quantification of NEO-PUFAs in *T. lutea* incubated under control, copper or H_2O_2 stress condition. Data are mean ± Sd (n=3 except for copper stress, n=2) expressed as ng/g dry weight. NaN stands for Not a Number because impossible value.

	CTL		Cu^{2+}		H_2O_2	
	Conc.	Sd	Conc.	Sd	Conc.	Sd
10-*epi*-10-F_{4t}-NeuroP	1.37e+02	1.24e+01	1.9e+02	NaN	1.75e+02	5.17e+01
10-F_{4t}-NeuroP	1.05e+02	1.03e+01	1.53e+02	NaN	1.32e+02	3.75e+01
13-*epi*-13-F_{4t}-NeuroP	2.82e+02	1.54e+01	3.12e+02	NaN	3.34e+02	7.12e+01
13-F_{4t}-NeuroP	4.33e+02	3.33e+01	5.05e+02	NaN	5.43e+02	1.25e+02
14 (*RS*)-14-F_{4t}-NeuroP	1.32e+02	1.58e+01	1.59e+02	NaN	1.67e+02	7.29e+01
16-B_1-PhytoP	9.88e+02	9.9e+01	1.01e+03	NaN	1.05e+03	1.69e+02
16 (*RS*)-16-A_1-PhytoP	3.24e+02	3.02e+01	5.87e+02	NaN	3.48e+02	3.93e+01
18-F_{3t}-IsoP	4.54e+00	1.13e+00	4.6e+00	NaN	2.46e+00	NaN
20-*epi*-20-F_{4t}-NeuroP	1.16e+02	1.53e+01	2.13e+02	NaN	1.44e+02	3.32e+01
20-F_{4t}-NeuroP	2.03e+02	2.08e+01	3.26e+02	NaN	2.56e+02	6e+01
4 (*RS*)-4-F_{3t}-NeuroP	1.35e+02	1.75e+01	2.61e+02	NaN	1.38e+02	1.53e+01
4 (*RS*)-4-F_{4t}-NeuroP	5.15e+02	3.87e+01	8.26e+02	NaN	6.01e+02	1.02e+02
5 (*RS*)-5-F_{2t}-IsoP	5.05e+00	6.35e-01	1.31e+01	NaN	6.1e+00	1.09e+00
5-F_{2c}-IsoP	6.33e+00	NaN	1.96e+01	NaN	9.03e+00	9.25e-01
7 (*RS*)-ST-Δ^{18}-11-dihomo-IsoF	4.18e+01	3.5e+00	7.85e+01	NaN	4.95e+01	1.22e+01
8-*epi*-8-F_{3t}-IsoP	1.24e+00	3.44e-01	2.43e+00	NaN	1.9e+00	9.39e-01
8-F_{3t}-IsoP	2.27e+00	4.48e-01	4.21e+00	NaN	3.64e+00	9.7e-01
9-*epi*-9-F_{1t}-PhytoP	2.37e+02	4.34e+01	5.75e+02	NaN	3.24e+02	7.12e+01
9-F_{1t}-PhytoP	4.07e+02	3.36e+01	7.3e+02	NaN	4.66e+02	6.59e+01
9-L_1-PhytoP	7.27e+02	8.22e+01	1.3e+03	NaN	7.59e+02	1.28e+02
ent-16-*epi*-16-F_{1t}-PhytoP	3.15e+02	2.88e+01	6.1e+02	NaN	3.61e+02	5.07e+01
ent-16-F_{1t}-PhytoP	3.81e+02	2.04e+01	6.82e+02	NaN	4.09e+02	6.66e+01
ent-16(*RS*)-13-*epi*-Δ^{14}-9-PhytoF	1.88e+02	1.86e+01	4.02e+02	NaN	2.1e+02	2.16e+01
ent-16(*RS*)-9-*epi*-ST-Δ^{14}-10-PhytoF	8.59e+02	8.45e+01	1.81e+03	NaN	1.02e+03	1.07e+02
ent-7(*RS*)-7-F_{2t}-dihomo-IsoP	3.26e+00	6.02e-01	1.37e+01	NaN	4.47e+00	1.48e+00
9-*epi*-9-D_{1t}-PhytoP	6.55e+01	1.09e+01	1.72e+02	NaN	9.46e+01	3.56e+01
ent-9-*epi*-9-D_{1t}-PhytoP	1.15e+02	2.49e+01	2.63e+02	NaN	1.42e+02	3.81e+01
ent-9(*RS*)-12-*epi*-ST-Δ^{10}-13-PhytoF	2.21e+02	1.89e+01	4.51e+02	NaN	2.51e+02	2.74e+01

The production of these molecules is in accordance with the fatty acid profile of *T. lutea* since ALA and DHA are the most abundant PUFAs measured in this alga [~~37, 40~~39, 42], and the content of their oxidized derivatives represented 97% of the total amount of identified isoprostanoids. Taking a closer look at the four main families of metabolites, amounts of ALA derivatives ranged from 0.07 µg/g (*ent*-9-D_{1t}-PhytoP) to 1 µg/g (16-B_1-PhytoP), and those of AA derivatives from 5 ng/g (5(*RS*)-5-F_{2t}-IsoP) to 6 ng/g (5-F_{2c}-IsoP). The content of EPA derivatives goes from 1.2 ng/g for the lowest (8-*epi*-8-F_{3t}-IsoP) to 4.5 ng/g for the highest (18-*epi*-18-F_{3t}-IsoP), and for DHA derivatives, from 0.1 µg/g for the lowest (10-*epi*-10-F_{4t}-NeuroP) to 0.5 µg/g for the highest (4(*RS*)-4-F_{4t}-NeuroP).

When assessing the impact of oxidative conditions, oxidized metabolite diversity remained unchanged. Furthermore, no variation in the isoprostanoid content of *T. lutea* was monitored after incubation in the presence of H_2O_2. In contrast, copper treatment had a strong effect: the content of 17 among the 38 oxidized derivatives increased under this stress condition. Two compounds were very significantly impacted as shown by the p-values adjusted for multiples comparison: 5-F_{2c}-IsoP ($p < 0.0005$), and *ent*-16-*epi*-16-F_{1t}-PhytoP ($p < 0.001$). To a lesser extent, changes in content of *ent*-16(*RS*)-9-*epi*-ST-Δ^{14}-10-PhytoF, *ent*-9(*RS*)-12-*epi*-ST-Δ^{10}-13-PhytoF, and 4(*RS*)-4-F_{3t}-$NeuroP_{DPAn\text{-}6}$ were also statistically supported ($p < 0.005$) (Tables S4). This concerned four of the six families of NEO-

PUFAs identified, i.e. those derived from ALA, EPA, DPA_{n-6}, and AdA, while the content of derivatives from EPA and DHA did not change significantly. Comparing the content of each of the four families between control and copper stress condition indicated an increase by 160%, 184%, 104% and 93% for derivatives of ALA, AA, AdA, and for DPA_{n-6} respectively, i.e. a two to three-fold increase in isoprostanoid content (Figure 4). The concentration of *ent*-9-D_{1t}-PhytoP, the metabolite from ALA with the highest content in the control condition (65 ng/g), reached a value of 172 ng/g after cupric stress. Similarly, the content of 5-F_{2c}-IsoP increased from 6 ng/g to 20 ng/g, of *ent*-7(*RS*)-F_{2t}-dihomo-IsoP from 3 ng/g to 14 ng/g, and of 4(*RS*)-4-F_{3t}-$NeuroP_{DPAn-6}$ from 135 ng/g to 260 ng/g. None of the inventoried compounds shown a decrease in content after applying any of the two oxidative stresses.

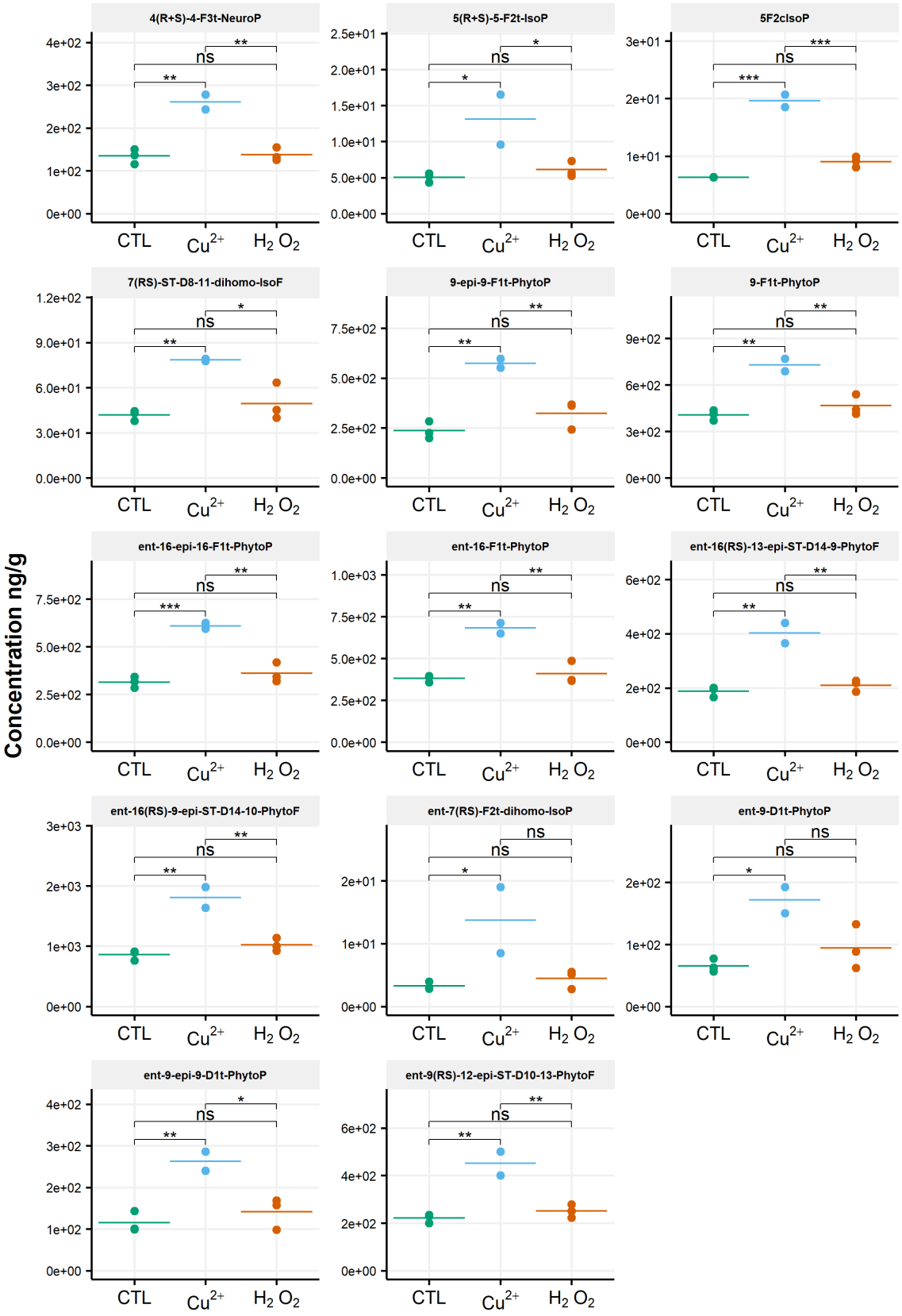

Figure 4. : Changes in content of selected isoprostanoids for the haptophyte *T. lutea* between control condition (CTL) and oxidative stress (Cu^{2+} and H_2O_2) conditions. Statistically relevant responses between control and stress conditions (one-way ANOVA) are indicated by asterisks: *, $p < 5 \times 10^{-2}$; **, $p < 5 \times 10^{-3}$; ***, $p < 5 \times 10^{-4}$; ns, not significant.

3.4. *Chaetoceros gracilis*

In this diatom, 28 different isoprostanoids were identified, derived from all the PUFAs mentioned above, except DPA_{n-6}, and accounted for 2.45 µg/g (Table 4).

Table 4. : Quantification of NEO-PUFAs in *C. gracilis* incubated under control, copper or H_2O_2 stress. Data are mean ± Sd (n=3) expressed as ng/g dry weight. NaN stands for Not a Number because impossible value.

	CTL		Cu^{2+}		H_2O_2	
	Conc.	Sd	Conc.	Sd	Conc.	Sd
10-*epi*-10-F_{4t}-NeuroP	5.24e+00	4.37e-01	6.23e+00	1.32e+00	5.68e+00	NaN
10-F_{4t}-NeuroP	3.28e+00	2.17e-01	3.97e+00	5.03e-01	8.23e+00	8.04e+00
13-*epi*-13-F_{4t}-NeuroP	1.1e+01	7.79e-01	1.43e+01	1.51e+00	2.47e+01	2.28e+01
13-F_{4t}-NeuroP	1.46e+01	1.88e+00	1.66e+01	3.6e+00	3.18e+01	2.58e+01
15-*epi*-15-F_{2t}-IsoP	1.32e+01	4.43e-01	1.6e+01	2.4e-01	1.93e+01	1.41e+01
15-F_{2t}-IsoP	9.32e+00	4.49e-01	1.08e+01	1.24e+00	1.47e+01	1.1e+01
16-B_1-PhytoP	4.38e+00	9.13e-01	7.04e+00	2.1e+00	4.22e+00	1.29e+00
18-F_{3t}-IsoP	6.35e+02	3.35e+01	7.67e+02	NaN	1.04e+03	7.92e+02
18-*epi*-18-F_{3t}-IsoP	3.62e+02	1.61e+01	4.28e+02	NaN	3.35e+02	NaN
20-*epi*-20-F_{4t}-NeuroP	9.38e+00	9.76e-01	1.03e+01	NaN	1.58e+01	1.15e+01
20-F_{4t}-NeuroP	1.07e+01	2.15e+00	1.03e+01	2.79e+00	1.77e+01	1.34e+01
4 (*RS*)-4-F_{4t}-NeuroP	2.27e+01	1.62e+00	2.32e+01	4.11e+00	2.39e+01	NaN
5-*epi*-5-F_{3t}-IsoP	6.03e+02	2.66e+01	6.61e+02	9.23e+01	5.69e+02	NaN
5 (*RS*)-5-F_{2t}-IsoP	3.51e+01	3.19e+00	4.14e+01	7.19e+00	6.11e+01	5.28e+01
5-F_{3t}-IsoP	4.71e+02	2.22e+01	4.77e+02	8.04e+01	4.93e+02	NaN
5-F_{2c}-IsoP	1.05e+02	3.71e+00	1.4e+02	2.01e+01	2.48e+02	1.8e+02
7 (*RS*)-ST-Δ^{18}-11-dihomo-IsoF	1.08e+01	7.54e-01	1.42e+01	8.02e-01	1.29e+01	2.66e+00
8-*epi*-8-F_{3t}-IsoP	5.75e+01	3.01e+00	6.37e+01	7.63e+00	5.6e+01	NaN
8-F_{3t}-IsoP	5.24e+01	2.05e+00	6.29e+01	7.24e+00	5.66e+01	NaN
9-F_{1t}-PhytoP	2.06e+00	1.36e-01	2.43e+00	8.89e-02	2.83e+00	1.29e+00
9-L_1-PhytoP	3.21e+00	5.87e-01	5.4e+00	1.53e+00	3.27e+00	9.2e-01
ent-16-*epi*-16-F_{1t}-PhytoP	1.44e+00	1.64e-01	1.84e+00	2.29e-01	2.04e+00	9.52e-01
ent-16(*RS*)-9-*epi*-ST-Δ^{14}-10-PhytoF	4.44e+00	3.54e-01	7.08e+00	1.33e+00	5.51e+00	1.59e+00
ent-9-*epi*-9-D_{1t}-PhytoP	3.96e+00	3.47e-01	6.51e+00	1.02e+00	7.54e+00	5.75e+00

Seven phytoprostanoids and phytofuranoides derived from ALA were observed, and represented 0.019 µg/g. The concentrations ranged from 1.4 ng/g (*ent*-16-*epi*-16-F_{1t}-PhytoP) to 4.4 ng/g (*ent*-16(*RS*)-9-*epi*-ST-Δ^{14}-10-PhytoF). Eight neuroprostanoids from DHA (0.077 µg/g), six EPA derivatives (2.2 µg/g), five AA derivatives (0.16 µg/g), and two AdA derivatives (0.011 µg/g) were also identified. DHA derivatives have contents ranging from 3.3 ng/g (10-F_{4t}-NeuroP) to 14.6 ng/g (13B(*RS*)-13-F_{4t}-NeuroP), while EPA derivatives accumulated from 52.4 ng/g (8-*epi*-8-F_{3t}-IsoP) to 535 ng/g (18-*epi*-18-F_{3t}-IsoP), and AA derivatives from 9.3 ng/g (15-F_{2t}-IsoP) to 105 ng/g (5-F_{2c}-IsoP). As it could be expected based on the high content of EPA found in *C. gracilis* [~~37, 41, 42~~39, 43, 44], the most abundant isoprostanoids identified in this species were derived from this PUFA, notably the diasteroisomer pair 5(*RS*)-5-F_{3t}-IsoP that accounted for approximately 42% (1.1 µg/g) of the total amount of oxidized metabolites measured.

For this alga, the qualitative profile remained mostly unchanged, similarly to the amounts of the individual molecules, between the control and the two oxidative stress conditions tested. The only exception was for the compound 18-F_{3t}-IsoP: it showed a slight significant difference in its concentration under Cu^{2+} stress condition, increasing from 362 ng/g to 428 ng/g ($p = 0.015$) (Figure 5) (Tables S4).

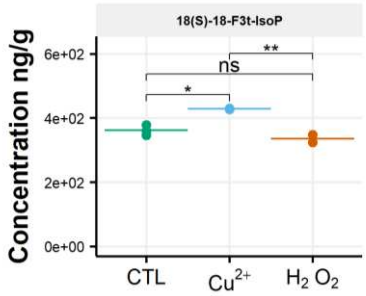

379

380 **Figure 5. :** Changes in content of selected isoprostanoids for the diatom *C. gracilis* between control
381 condition (CTL) and oxidative stress (Cu^{2+} and H_2O_2) conditions. Statistically relevant responses
382 between control and stress conditions (one-way ANOVA) are indicated by asterisks: *, $p < 5 \times 10^{-2}$;
383 **, $p < 5 \times 10^{-3}$; ns, not significant.

384 ***3.5.** Phaeodactylum tricornutum*

385 In this diatom, 21 different oxidized metabolites were identified and quantified, for a total of
386 0.32 µg/g. No derivatives of DPA_{n-6} were observed under any conditions. ALA derivatives
387 represented the main isoprostanoids in term of diversity with 12 metabolites (six PhytoPs and six
388 PhytoFs), and also in term of content (0.21 µg/g. i.e. 66% of the total amount). Concentrations of ALA
389 oxidized metabolites were comprised within a range of 2.6 ng/g (with *ent*-16(*RS*)-13-*epi*-ST-Δ^{14}-9-
390 PhytoF) to 44.2 ng/g (9-F_{1t}-PhytoP). The second most abundant derivatives were produced from EPA,
391 with four metabolites that accounted for 0.09 µg/g. The dynamic range was from 1.2 ng/g for (8-*epi*-
392 8-F_{3t}-IsoP to 47 ng/g for (5(*R*)-5-F_{3t}-IsoP). One single isoprostanoid from AA was identified (5-F_{2c}-IsoP;
393 13 ng/g), two from AdA (7(*RS*)-ST-Δ^{8}-11-dihomo-IsoF epimers; 5 ng/g), and finally two from DHA
394 (4(*RS*)-4-F_{4t}-NeuroP epimers; 2 ng/g). No oxidized derivatives of DPA_{n-6} were found, as previously
395 stated for the other diatom *C. gracilis* (Table 5). As already mentioned for *T. lutea* and *C. gracilis*, *P.*
396 *tricornutum* produced isoprostanoids in accordance with its PUFA profile that contain mainly ALA
397 and EPA [~~37, 43~~39, 45].

398 **Table 5. :** Quantification of NEO-PUFAs in *P. tricornutum* incubated under control, copper or H2O2
399 stress condition. Data are mean ± Sd (n=3) expressed as ng/g dry weight. NaN stands for Not a
400 Number because impossible values.

	CTL		*Cu^{2+}*		*H_2O_2*	
	Conc.	Sd	Conc.	Sd	Conc.	Sd
16-B_1-PhytoP	1.51e+01	1.38e+00	4.27e+01	5.94e+00	3.8e+00	1.23e+00
4 (*RS*)-4-F_{4t}-NeuroP	1.84e+00	4.57e-02	2.91e+00	1.69e-01	2.31e+00	5.18e-01
5-*epi*-5-F_{3t}-IsoP	4.71e+01	2.74e+00	9.99e+01	1.4e+01	8.66e+01	4.94e+01
5-F_{3t}-IsoP	3.37e+01	2.07e+00	7.29e+01	8.36e+00	5.79e+01	3.24e+01
5-F_{2c}-IsoP	1.3e+01	1.02e+00	2.52e+01	3.05e+00	1.42e+01	2.78e+00
7 (*RS*)-ST-Δ^{18}-11-dihomo-IsoF	5.41e+00	5.54e-01	1.11e+01	1.66e+00	5.14e+00	1.69e+00
8-*epi*-8-F_{3t}-IsoP	6.72e+00	7.59e-01	1.2e+01	1.83e+00	1.08e+01	4.19e+00
8-F_{3t}-IsoP	3.92e+00	3.04e-01	7.99e+00	9.11e-01	6.92e+00	3.48e+00
9-F_{1t}-PhytoP	4.42e+01	4.36e+00	5.25e+01	3.05e+00	3.72e+01	3.93e+00
9-L_1-PhytoP	1.23e+01	1.13e+00	3.4e+01	4.63e+00	3.25e+00	8.46e-01
ent-16-*epi*-16-F_{1t}-PhytoP	3.15e+01	3.19e+00	3.71e+01	2.1e+00	2.63e+01	2.54e+00
ent-16-F_{1t}-PhytoP	8.1e+01	8.05e+00	9.09e+01	4.69e+00	6.73e+01	7.15e+00
ent-16(*RS*)-13-*epi*-Δ^{14}-9-PhytoF	2.64e+00	3.12e-01	7.01e+00	NaN	1.06e+00	2.68e-01
ent-16(*RS*)-9-*epi*-ST-Δ^{14}-10-PhytoF	2.02e+01	2.46e+00	4.4e+01	4.61e+00	5.78e+00	1.94e+00
ent-9-*epi*-9-D_{1t}-PhytoP	9.18e-01	1.82e-01	2.4e+00	3.92e-01	7.83e-01	4.26e-01
ent-9(*RS*)-12-*epi*-ST-Δ^{10}-13-PhytoF	4.53e+00	7.44e-01	1.17e+01	1.65e+00	3.58e+00	8.82e-01

401

The isoprostanoid profile of the diatom *P. tricornutum* was strongly influenced by copper treatment, in contrast to what was observed for the other diatom *C. gracilis* (Figure 6).

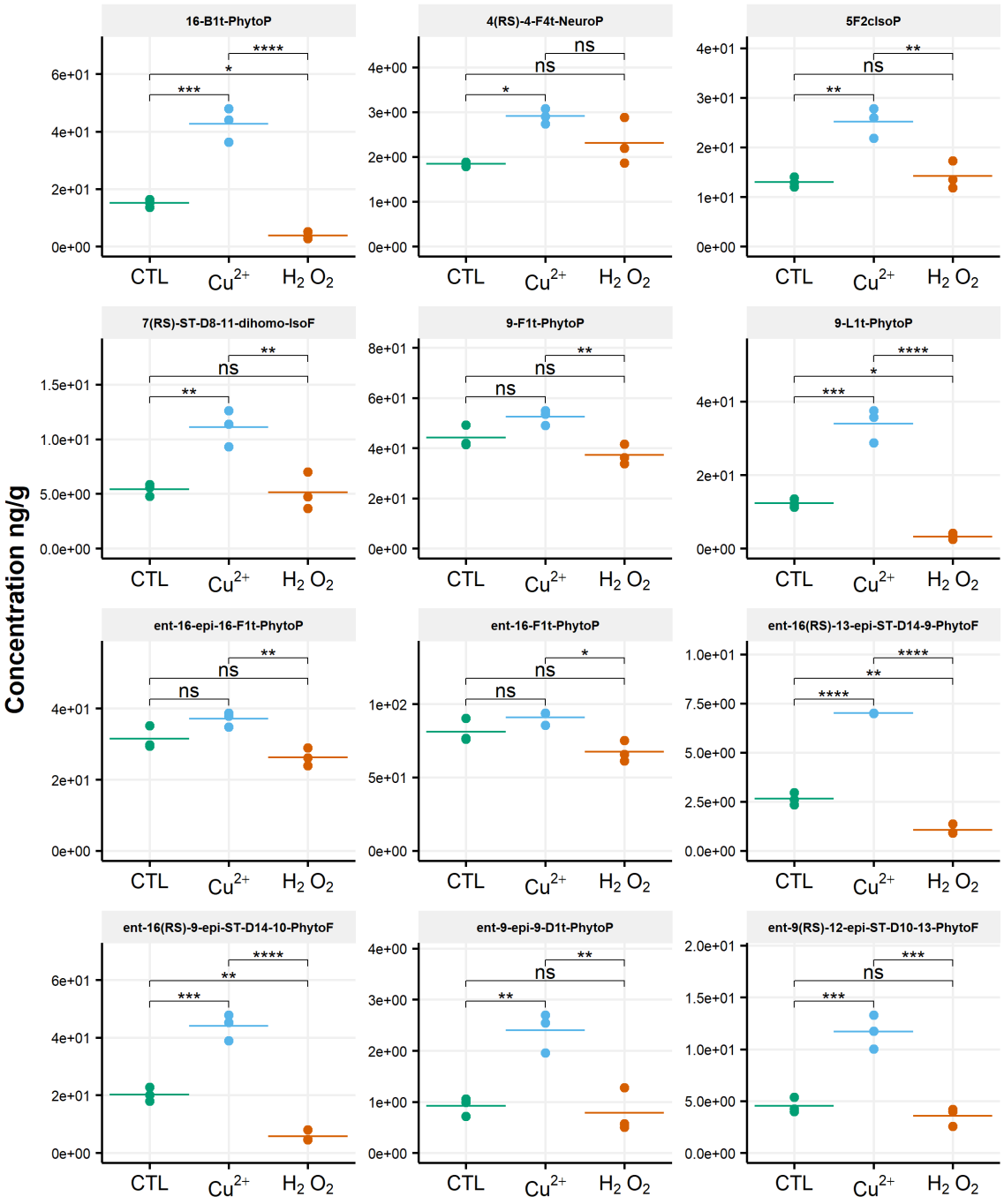

Figure 6. : Changes in content of selected isoprostanoids for the diatom *P. tricornutum* between control condition (CTL) and oxidative stress (Cu^{2+} and H_2O_2) conditions. Statistically relevant responses between control and stress conditions (one-way ANOVA) are indicated by asterisks: *, $p < 5 \times 10^{-2}$; **, $p < 5 \times 10^{-3}$; ***, $p < 5 \times 10^{-4}$; ns, not significant.

A significant increase in the content of 14 metabolites among the 21 identified was observed (Tables S4). This was particularly significant for *ent*-16(*RS*)-13-*epi*-ST-Δ^{14}-9-PhytoF ($p < 0.00005$) with a concentration of 2.6 ng/g in control condition and 7 ng/g under copper stress condition. Compounds

16-B$_1$-PhytoP, 9-L$_1$-PhytoP, *ent*-16(*RS*)-9-*epi*-ST-Δ^{14}-10-PhytoF and *ent*-9(*RS*)-12-*epi*-ST-Δ^{10}-13-PhytoF were also strongly impacted by copper with significant modifications in content ($p < 0.0005$). The concentrations of these different metabolites increased from 15 ng/g to 43 ng/g, 12 ng/g to 34 ng/g, 20 ng/g to 44 ng/g and 4.5 ng/g to 12 ng/g respectively. The amounts of derivatives of ALA enhanced by 94%, of AA by 94%, of AdA by 105%, and of DHA by 58%, representing on average a twofold increase in isoprostanoids content. No change in isoprostanoids for which EPA is the precursor was observed. No metabolite showed a decrease in content.

Surprisingly, we monitored lower levels of isoprostanoids under H_2O_2 stress compared to control condition for *P. tricornutum*. The content of the two epimers series derived from ALA oxidation, *ent*-16(*RS*)-13-*epi*-ST-Δ^{14}-9-PhytoF and *ent*-16(*RS*)-9-*epi*-ST-Δ^{14}-10-PhytoF, decreased by factor two and four respectively ($p < 0.005$). In the same vein, amounts of 16-B$_1$-PhytoP and 9-L$_1$-PhytoP were four times lower under H_2O_2 stress condition compared to the control ($p < 0.05$).

4. Discussion

There is an increasing interest in studying oxylipin metabolism in marine microalgae. This is supported by recent publications describing profiles of enzymatically produced oxidized derivatives of PUFAs, and their potential physiological roes [17, ~~44-47~~46-49]. So far, little emphasis has been put on biosynthesis, by eukaryotic phytoplankton, of isoprostanoids, i.e. oxylipins produced non-enzymatically by reaction of ROS with the double bonds of PUFAs. In this context, and to our knowledge, the current study is the first to report the production of phytoprostanes, phytofurans, isoprostanes (serie 2 and 3), and neuroprostanes, all derived from PUFA precursors that include ALA, AdA, EPA, DPA$_{n-6}$, and DHA, in the cryptophyte *R. salina*, the haptophyte *T. lutea*, and the diatom *C. gracilis*. In addition, it extends the repertoire of isoprostanoids recently published for another diatom, *P. tricornutun* [19]. Under laboratory culture growth conditions, a good correlation between the presence of PUFAs and the biosynthesis of NEO-PUFAs was observed. We have already noticed this in our previous study on macroalgae, notably with the *Rhodophyta* species, *Grateloupia turuturu* Yamada, known to be rich in AA and which produced significant amounts of oxidized AA metabolites [18]. The four microalgae investigated in the present study exhibited different levels of diversity, as well as marked differences in the amount of isoprostanoids produced. A high content of ALA derivatives was quantified in *R. salina*. The diatom *P. tricornutum*, which appeared to contain lower amounts of oxidized derivatives compared to the other microalgae used, was mostly rich in AA derivatives. The diatoms *C. gracilis* shown profiles rich in NEO-PUFAs produced from EPA. High content of ALA and DHA derivatives were identified in *T. lutea*. After exposure to oxidative stress conditions, changes in the diversity and amounts of isoprostanoids produced were species and stress dependent. Under copper stress, no strong variations were observed in *R. salina* and *C. gracilis*, whereas a significant increase in the production of C18-, C20- and C22- derived isoprostanoids was monitored in *T. lutea*. and *P. tricornutum*. H_2O_2 stress had different impacts. NEO-PUFA concentrations remained unchanged for *C. gracilis* and *T. lutea*, whereas profiles and contents where altered in *R. salina* and *P. tricornutum*, notably for the ALA oxidized derivatives. Changes in phytoprostanes derived from ALA have been recently observed in this latter alga under H_2O_2 treatment slightly different from the condition considered in our analysis (1 mM for 24 hours), i.e. 0.25 and 0.75 mM of H_2O_2 applied during 48 h [19]. Interestingly, this study identified a number of isoprostanoids derived from ALA, ARA, EPA, and DHA which levels were differentially affected after oxidative stress. The authors have studied the influence of nine synthetic isoprostanoids,

applied in the micromolar range, on the physiology and lipid metabolism of *P. tricornutum.* They observed an induction of the accumulation of triacylglycerols (storage lipids), and a reduction of growth without alteration of photosynthesis. Such study, describing the characterization of non-enzymatic oxylipins in *P. tricornutum*, and suggesting physiological roles for these molecules, pave the way to better understand their importance in the biology of marine microalgae.

In the context of research on microalgal biorefinery, numerous studies were conducted on culture parameters and have shown to impact the production of PUFAs, such as light ~~[48],~~ ~~macronutrient depletion~~ [50], macronutrient depletion [~~49, 50~~51, 52], temperature ~~[51] or salinity~~ [53] or salinity [~~52~~54]. Nitrogen depletion or salinity stress, for instance, were shown to induce oxidative stress and significant changes in PUFAs production ~~[49], but little is known about the impact of these abiotic parameters on oxidized PUFA derivatives.~~[51], but little is known about the impact of these abiotic parameters on oxidized PUFA derivatives. Under laboratory culture growth conditions, our study showed that isoprostanoid profiles present good correlations with PUFA contents, and that their production could be increased in *T. lutea*, *P. tricornutum*, and *R. salina* by applying direct oxidative stress, either through copper or H_2O_2 addition. According to previous studies on lipid metabolism regulation, these results suggest that culture condition manipulation could also be an interesting field to be explored for improving biotechnological production of microalgal isoprostanoids.

From a more methodological point of view, it is worth underlining the sensitivity of the measurements since we have managed to measure metabolites present in very small quantities. Indeed, considering the case of *P. tricornutum* and of its lowest represented isoprostanoid (8-*epi*-8-F_{3t}-IsoP) presents at approximately 1 ng/g, it is satisfying to detect and reliably quantify molecules at such very low levels. With LODs ranging between 0.16 ng/g and 0.63 ng/g, and LOQs comprised between 0.16 ng/g and 1.25 pg/g, we can consider the method as sensitive. Interestingly, these low detection limits enable to detect and quantify a great diversity of metabolites. To our knowledge, the 38 oxidized metabolites detected in *T. lutea* represent the highest diversity of isoprostanoids identified from a given organisms so far, including plants and animals. This number of 38 isoprostanoids is close to the number of molecules for which we currently have standards for our targeted lipidomics method (47 metabolites). However, we cannot ensure that these undetected compounds were absent. Some of the missing metabolites may be present in amounts lower than our LODs/LODs, or may be produced but masked by other molecules from the matrix. To overcome these two issues, it is possible to foresee improving sample preparation, and also the chromatographic procedure by working on the choice of column, solvents, and gradient. Furthermore, it is important to emphasize that more than 38 isoprostanoids may be present in the microalgae studied, but could not be identified because our analysis is based on a targeted lipidomics approach, and thus only detects the metabolites present in the analytical method. Therefore, we think it is important to consider extending the library of isoprostanoid/oxylipin standards through synthesis of new molecules by chemists, as well as to adopt an untargeted lipidomics method [~~53, 54~~55, 56] to expand investigation of algal isoprostanoids in the future. Another important observation is that there is a very large difference in the concentration of NEO-PUFAs in the four species investigated, although this can be partly smoothed out by applying the correction factors of extraction yield and matrix effect.

Finally, recent studies have shown promising biological activities for PhytoPs, IsoPs and

NeuroPs [16, ~~55~~57]. For instance, Minghetti et al. showed the ability of the phytoprostane B_1-PhytoP, through novel mechanisms involving PPAR-γ, to specifically affect immature brain cells, such as neuroblasts and oligodendrocyte progenitors, thereby conferring neuroprotection against oxidant injury and promoting myelination ~~[56].~~[58]. Duda et al. showed the role, also as lipid mediator, of some phytoprostanes in the immediate effector phase of allergic inflammation [~~36~~38]. More recently, the work of Lee et al. put forward the hypothesis of the neuroprotective effect of 4-F_{4t}-NeuroP in cellular and animal models ~~[57].~~[59]. Early studies on the cardiovascular system demonstrated that AA oxidized derivatives induced platelet aggregation or show hypertensive effect [~~58, 59~~60, 61]. More recent studies showed that IsoPs and NeuroPs have beneficial effects in cardiovascular disease. Indeed, Leguennec et al. revealed that the lipid mediator 4-F_{4t}-NeuroP derived from non-enzymatic peroxidation of DHA has anti-arrhythmia effect in ventricular cardiomyocytes and in post-myocardial infarcted mice ~~[60].~~[62]. They also demonstrated the capability of such derivative to prevent and protect rat myocardium from reperfusion damages following occlusion (ischemia) [~~61~~63]. Due to high amounts quantified in some of the tested microalgae, especially after copper exposure, it may be worth exploring these organisms as a potential natural resource for production of isoprostanoids. Extraction of these NEO-PUFAs from marine microalgae could be an interesting alternative to current production by complex chemical syntheses, as are macroalgae. In this context, further work should focus on assessing how culture conditions alter isoprostanoid content and diversity in selected algae, towards enhancing production for future extraction from natural resources.

5. Conclusions

The current investigation aimed at profiling isoprostanoids by micro-LC-MS/MS in selected marine microalgae belonging to different lineages: the cryptophyte *Rhodomonas salina*, the haptophyte *Tisochrysis lutea*, and the diatoms *Phaeodactylum tricornutum* and *Chaetoceros gracilis*. To our knowledge, this is the first report of such a wide variety of NEO-PUFAs produced in microalgae. For instance, our analysis allowed the detection of PUFAs oxidized derivatives never reported so far, and we detected no less than 38 different metabolites in *T. lutea*. Our study is also the first to establish a link between significant changes in the isoprostanoid profiles of some selected microalgae and heavy metal stress. It also highlights the impact of hydrogen peroxide stress on NEO-PUFAs in some cases. Based on recent studies showing promising biological activities for NEO-PUFAs and due to high amounts quantified in some of the tested microalgae, further work should focus on assessing how manipulating culture conditions could enhance the production of isoprostanoids in selected species, notably by targeting the PUFAs biosynthetic pathway.

Supplementary Materials:

Figure S1: Chromatogram of selected reaction monitoring (SRM) of metabolites detected in *Chaetoceros gracilis*.

Figure S2: Distribution of oxidized metabolites (sum of concentrations) classified according to the original PUFAs in the four species studied.

Table S1: Selected reaction monitoring (SRM) of the isoprostanes derived from polyunsaturated fatty acids.

Table S2: Standards calibration curves

Tables S3a and Sb: Determination of matrix effect and extraction efficiency for isoprostanoids' extraction from the four species studied : (a) *P. tricornutum* and *T. lutea* ; (b) *C. gracilis* and *R. salina*. Each data point is the mean of six replicates.

Tables S4: Statistical results expressed with one-way ANOVA and Post-Hoc test analysis for the four species studied. Statistically relevant responses between control and stress conditions (one-way ANOVA) are indicated by asterisks: *, $p < 5 \times 10^{-2}$; **, $p < 5 \times 10^{-3}$; ***, $p < 5 \times 10^{-4}$; ns, not significant.

Author Contributions: C.V., C.O., T.D., P.P., T.T. and C.L. designed and managed the study. C.V. and T.T. wrote the manuscript. C.O., J.V., T.D., J-M.G., A.G., V.B-P., P.P. and C.L. contributed to the manuscript corrections. A.R., B.Z., G.R., A.L-M. analysed NEO-PUFAs contents. C.V., G.R., P.P., T.T. and C.L. conducted the study at the experimental facilities.

Funding: This work received financial support from EMBRC France (European Marine Biological Resource Centre) through a call of projects 2015. This project was also partly funded by IDEALG (France: ANR-10- BTBR-04), and by the European Joint Programming Initiative "A Healthy Diet for a Healthy Life" (JPI HDHL – ANR-15-HDHL-0003).

Acknowledgments: We thank colleagues of the Marine Biological Resource Centre at the Station Biologique de Roscoff, and especially Ronan Garnier, for providing technical help to implement microalgal cultivation, and those from Merabomer-Corsaire for access to sample extraction facilities. We also thanks colleagues of MAMMA platform.

Conflicts of Interest: The funders had no role in the design of the study; in the collection, analyses, or interpretation of data; in the writing of the manuscript, or in the decision to publish the results.

References

1. Worden, A.Z., M.J. Follows, S.J. Giovannoni, S. Wilken, A.E. Zimmerman, and P.J. Keeling, Environmental science. Rethinking the marine carbon cycle: factoring in the multifarious lifestyles of microbes. *Science* **2015**, *347* (6223), 1257594. 10.1126/science.1257594.
2. Ebenezer, V., L.K. Medlin, and J.S. Ki, Molecular detection, quantification, and diversity evaluation of microalgae. *Mar Biotechnol (NY)* **2012**, *14* (2), 129-42. 10.1007/s10126-011-9427-y.
3. Brodie, J., C.X. Chan, O. De Clerck, J.M. Cock, S.M. Coelho, C. Gachon, A.R. Grossman, T. Mock, J.A. Raven, A.G. Smith, H.S. Yoon, and D. Bhattacharya, The Algal Revolution. *Trends Plant Sci* **2017**, *22* (8), 726-738. 10.1016/j.tplants.2017.05.005.
4. Venkata Mohan, S., M. Hemalatha, D. Chakraborty, S. Chatterjee, P. Ranadheer, and R. Kona, Algal biorefinery models with self-sustainable closed loop approach: Trends and prospective for blue-bioeconomy. *Bioresource Technology* **2020**, *295*, 10.1016/j.biortech.2019.122128.
5. Castro, L.F., D.R. Tocher, and O. Monroig, Long-chain polyunsaturated fatty acid biosynthesis in chordates: Insights into the evolution of Fads and Elovl gene repertoire. *Prog Lipid Res* **2016**, *62*, 25-40. 10.1016/j.plipres.2016.01.001.
6. Calder, P.C., Very long chain omega-3 (n-3) fatty acids and human health. *Eur. J. Lipid Sci. Technol.* **2014**, *116* (10), 1280-1300. 10.1002/ejlt.201400025.
7. Calder, P.C., Very long-chain n-3 fatty acids and human health: fact, fiction and the future. *Proc Nutr Soc* **2018**, *77* (1), 52-72. 10.1017/S0029665117003950.
8. Delgado-Lista, J., P. Perez-Martinez, J. Lopez-Miranda, and F. Perez-Jimenez, Long chain omega-3 fatty acids and cardiovascular disease: a systematic review. *Br J Nutr* **2012**, *107 Suppl 2*, S201-13. 10.1017/S0007114512001596.
9. Innis, S.M., Dietary (n-3) fatty acids and brain development. *J Nutr* **2007**, *137* (4), 855-9. 10.1093/jn/137.4.855.

582 10. Campoy, C., M.V. Escolano-Margarit, T. Anjos, H. Szajewska, and R. Uauy, Omega 3 fatty acids on
583 child growth, visual acuity and neurodevelopment. *Br J Nutr* **2012**, *107 Suppl 2*, S85-106.
584 10.1017/S0007114512001493.
585 11. Hilgendorf, K.I., C.T. Johnson, A. Mezger, S.L. Rice, A.M. Norris, J. Demeter, W.J. Greenleaf, J.F. Reiter,
586 D. Kopinke, and P.K. Jackson, Omega-3 Fatty Acids Activate Ciliary FFAR4 to Control Adipogenesis.
587 *Cell* **2019**, *179* (6), 1289-1305 e21. 10.1016/j.cell.2019.11.005.
588 12. Tocher, D.R., M.B. Betancor, M. Sprague, R.E. Olsen, and J.A. Napier, Omega-3 Long-Chain
589 Polyunsaturated Fatty Acids, EPA and DHA: Bridging the Gap between Supply and Demand. *Nutrients*
590 **2019**, *11* (1), 89. 10.3390/nu11010089.
591 13. Diao, J., X. Song, T. Guo, F. Wang, L. Chen, and W. Zhang, Cellular engineering strategies toward
592 sustainable omega-3 long chain polyunsaturated fatty acids production: State of the art and
593 perspectives. *Biotechnology Advances* **2020**, *40*, 107497. 10.1016/j.biotechadv.2019.107497.
594 14. Napier, J.A., R.-E. Olsen, and D.R. Tocher, Update on GM canola crops as novel sources of omega-3 fish
595 oils. *Plant Biotechnology Journal* **2019**, *17* (4), 703-705. 10.1111/pbi.13045.
596 15. Jahn, U., J.-M. Galano, and T. Durand, Beyond Prostaglandins—Chemistry and Biology of Cyclic
597 Oxygenated Metabolites Formed by Free-Radical Pathways from Polyunsaturated Fatty Acids.
598 *Angewandte Chemie International Edition* **2008**, *47* (32), 5894-5955. 10.1002/anie.200705122.
599 16. Galano, J.M., Y.Y. Lee, C. Oger, C. Vigor, J. Vercauteren, T. Durand, M. Giera, and J.C. Lee, Isoprostanes,
600 neuroprostanes and phytoprostanes: An overview of 25years of research in chemistry and biology.
601 *Progress in lipid research* **2017**, *68*, 83-108. 10.1016/j.plipres.2017.09.004.
602 17. Barbosa, M., J. Collado-Gonzalez, P.B. Andrade, F. Ferreres, P. Valentao, J.M. Galano, T. Durand, and
603 A. Gil-Izquierdo, Nonenzymatic alpha-Linolenic Acid Derivatives from the Sea: Macroalgae as Novel
604 Sources of Phytoprostanes. *Journal of agricultural and food chemistry* **2015**, *63* (28), 6466-74.
605 10.1021/acs.jafc.5b01904.
606 18. Vigor, C., G. Reversat, A. Rocher, C. Oger, J.M. Galano, J. Vercauteren, T. Durand, T. Tonon, C. Leblanc,
607 and P. Potin, Isoprostanoids quantitative profiling of marine red and brown macroalgae. *Food Chem*
608 **2018**, *268*, 452-462. 10.1016/j.foodchem.2018.06.111.
609 19. Lupette, J., A. Jaussaud, C. Vigor, C. Oger, J.M. Galano, G. Reversat, J. Vercauteren, J. Jouhet, T. Durand,
610 and E. Marechal, Non-enzymatic synthesis of bioactive isoprostanoids in the diatom Phaeodactylum
611 following oxidative stress. *Plant Physiol* **2018**, *178*, 1344-1357. 10.1104/pp.18.00925.
612 20. Kovac, D.J., J.B. Simeunovic, O.B. Babic, and A.C. Misan, Algae in food and feed. *Food & Feed research*
613 **2013**, *40* (1), 21-32.
614 21. Chauton, M.S., K.I. Reitan, N.H. Norsker, R. Tveterås, and H.T. Kleivdal, A techno-economic analysis
615 of industrial production of marine microalgae as a source of EPA and DHA-rich raw material for
616 aquafeed: Research challenges and possibilities. *Aquaculture* **2015**, *436*, 95-103.
617 10.1016/j.aquaculture.2014.10.038.
618 22. Kumari, P., M. Kumar, C.R.K. Reddy, and B. Jha, *Algal lipids, fatty acids and sterols*, in *Functional*
619 *Ingredients from Algae for Foods and Nutraceuticals*, H. Dominguez, Editor. **2013**, Woodhead Publishing.
620 p. 87-134.
621 23. Oger, C., Y. Brinkmann, S. Bouazzaoui, T. Durand, and J.M. Galano, Stereocontrolled access to
622 isoprostanes via a bicyclo[3.3.0]octene framework. *Organic letters* **2008**, *10* (21), 5087-90.
623 10.1021/ol802104z.

24. Oger, C., V. Bultel-Ponce, A. Guy, T. Durand, and J.M. Galano, Total synthesis of isoprostanes derived from AdA and EPA. *Eur. J. Org. Chem.* **2012**, *2012* (13), 2621-2634.
25. Guy, A., C. Oger, J. Heppekausen, C. Signorini, C. De Felice, A. Fürstner, T. Durand, and J. Galano, Oxygenated metabolites of n-3 polyunsaturated fatty acids as potential oxidative stress biomarkers: total synthesis of 8-F3t-IsoP, 10-F4t-NeuroP and [D4]-10-F4t-NeuroP. *Chem. Eur. J.* **2014**, *20* (21), 6374-80.
26. Cuyamendous, C., K.S. Leung, T. Durand, J.C. Lee, C. Oger, and J.M. Galano, Synthesis and discovery of phytofurans: metabolites of alpha-linolenic acid peroxidation. *Chemical communications* **2015**, *51* (86), 15696-9. 10.1039/c5cc05736a.
27. Lananan, F., A. Jusoh, N. Ali, S.S. Lam, and A. Endut, Effect of Conway Medium and f/2 Medium on the growth of six genera of South China Sea marine microalgae. *Bioresour Technol* **2013**, *141*, 75-82. 10.1016/j.biortech.2013.03.006.
~~28~~28. Heydarizadeh, P., W. Boureba, M. Zahedi, B. Huang, B. Moreau, E. Lukomska, A. Couzinet-Mossion, G. Wielgosz-Collin, V. Martin-Jézéquel, G. Bougaran, J. Marchand, and B. Schoefs, Response of CO2-starved diatom Phaeodactylum tricornutum to light intensity transition. *Philosophical Transactions of the Royal Society B: Biological Sciences* **2017**, *372* (1728), 20160396. 10.1098/rstb.2016.0396.
29. del Pilar Sánchez-Saavedra, M., A.N. Maeda-Martínez, and S. Acosta-Galindo, Effect of different light spectra on the growth and biochemical composition of Tisochrysis lutea. *Journal of Applied Phycology* **2016**, *28* (2), 839-847. 10.1007/s10811-015-0656-8.
30. Team, R.D.C., R: A language and environment for statistical computing. R Foundation for Statistical Computing **2008**, ISBN 3-900051-07-0~~,~~ http://www.R-project.org.
~~29~~31. Wickham, H., M. Averick, J. Bryan, W. Chang, L. D'Agostino McGowan, R. François, G. Grolemund, A. Hayes, L. Henry, J. Hester, M. Kuhn, T. Thomas Lin Pedersen, E. Miller, S. Milton Bache, K. Müller, J. Ooms, D. Robinson, D. Paige Seidel, V. Spinu, K. Takahashi, D. Vaughan, C. Wilke, K. Woo, and H. Yutani, Welcome to the tidyverse. *Journal of Open Source Software* **2019**, *4* (43), _10.21105/joss.01686.
~~30~~32. Zhu , H., T. Travison , T. Tsai , W. Beasley, Y. Xie, G. Yu, S. Laurent, R. Shepherd, Y. Sidi, B. Salzer, G. Gui, E. Fan, and D. Murdoch, kableExtra: Construct Complex Table with 'kable' and Pipe Syntax. R – package version 1.1.0. **2019**, https://CRAN.R-project.org/package=kableExtra.
~~31~~33. Kassambara, K., rstatix: Pipe-Friendly Framework for Basic Statistical Tests. R package version 0.4.0. . **2020**, https://CRAN.R-project.org/package=rstatix.
~~32~~34. Leung, K.S., X. Chen, W. Zhong, A.C. Yu, and C.Y. Lee, Microbubble-mediated sonoporation amplified lipid peroxidation of Jurkat cells. *Chem Phys Lipids* **2014**, *180*, 53-60. 10.1016/j.chemphyslip.2014.02.004.
~~33~~35. Dupuy, A., P. Le Faouder, C. Vigor, C. Oger, J.M. Galano, C. Dray, J.C. Lee, P. Valet, C. Gladine, T. Durand, and J. Bertrand-Michel, Simultaneous quantitative profiling of 20 isoprostanoids from omega-3 and omega-6 polyunsaturated fatty acids by LC-MS/MS in various biological samples. *Analytica chimica acta* **2016**, *921*, 46-58. 10.1016/j.aca.2016.03.024.
~~34~~36. Yonny, M.E., A. Rodriguez Torresi, C. Cuyamendous, G. Reversat, C. Oger, J.M. Galano, T. Durand, C. Vigor, and M.A. Nazareno, Thermal Stress in Melon Plants: Phytoprostanes and Phytofurans as Oxidative Stress Biomarkers and the Effect of Antioxidant Supplementation. *Journal of agricultural and food chemistry* **2016**, *64* (44), 8296-8304. 10.1021/acs.jafc.6b03011.
~~35~~37. Ruesgas-Ramón, M., M. Figueroa-Espinoza, E. Durand, M. Suárez-Quiroz, O. González-Ríos, A. Rocher, G. Reversat, J. Vercauteren, C. Oger, J. Galano, T. Durand, and C. Vigor, Identification and

quantification of phytoprostanes and phytofurans of coffee and cocoa by- and co-products. *Food Funct.* **2019**, *10* (10), 6882-6891. 10.1039/c9fo01528k.

~~36~~38. Gonzalez Roldan, N., R. Engel, S. Dupow, K. Jakob, F. Koops, Z. Orinska, C. Vigor, C. Oger, J.M. Galano, T. Durand, U. Jappe, and K.A. Duda, Lipid Mediators From Timothy Grass Pollen Contribute to the Effector Phase of Allergy and Prime Dendritic Cells for Glycolipid Presentation. *Front Immunol* **2019**, *10*, 974. 10.3389/fimmu.2019.00974.

~~37~~39. Jónasdóttir, S.A.-O., Fatty Acid Profiles and Production in Marine Phytoplankton. LID - 10.3390/md17030151 [doi] LID - 151. *Mar Drugs* **2019**, *17* (3), 151. 10.3390/md17030151.

~~38~~40. Fernández-Reiriz, M.J., A. Perez-Camacho, M.J. Ferreiro, J. Blanco, M. Planas, M.J. Campos, and U. Labarta, Biomass production and variation in the biochemical profile (total protein, carbohydrates, RNA, lipids and fatty acids) of seven species of marine microalgae. *Aquaculture* **1989**, *83* (1), 17-37. 10.1016/0044-8486(89)90057-4.

~~39~~41. Guevara, M., R. Bastardo L Fau - Cortez, B. Cortez R Fau - Arredondo-Vega, L. Arredondo-Vega B Fau - Romero, P. Romero L Fau - Gómez, and P. Gómez, Rhodomonas salina (Cryptophyta) pastes as feed for Brachionus plicatilis (Rotifera). *RevBiol Trop* **2011**, *59* (4), 1503-15.

~~40~~42. Huang, B., J. Marchand, S. Thiriet-Rupert, G. Carrier, B. Saint-Jean, E. Lukomska, B. Moreau, A. Morant-Manceau, G. Bougaran, and V. Mimouni, Betaine lipid and neutral lipid production under nitrogen or phosphorus limitation in the marine microalga Tisochrysis lutea (Haptophyta). *Algal Research* **2019**, *40*, 101506. 10.1016/j.algal.2019.101506.

~~41~~43. Volkman, J.K., S.W. Jeffrey, P.D. Nichols, G.I. Rogers, and C.D. Garland, Fatty acid and lipid composition of 10 species of microalgae used in mariculture. *Journal of Experimental Marine Biology and Ecology* **1989**, *128* (3), 219-240. 10.1016/0022-0981(89)90029-4.

~~42~~44. Pratiwi, A.R., D. Syah, L. Hardjito, L.M.G. Panggabean, and M.T. Suhartono, Fatty Acid Synthesis by Indonesian Marine Diatom, Chaetoceros gracilis. *HAYATI Journal of Biosciences* **2009**, *16* (4), 151-156. 10.4308/hjb.16.4.151.

~~43~~45. Cui, Y., S.R. Thomas-Hall, and P.M. Schenk, Phaeodactylum tricornutum microalgae as a rich source of omega-3 oil: Progress in lipid induction techniques towards industry adoption. *Food Chemistry* **2019**, *297*, 124937. 10.1016/j.foodchem.2019.06.004.

~~44~~46. Di Dato, V., I. Orefice, A. Amato, C. Fontanarosa, A. Amoresano, A. Cutignano, A. Ianora, and G. Romano, Animal-like prostaglandins in marine microalgae. *The ISME Journal* **2017**, *11* (7), 1722-1726. 10.1038/ismej.2017.27.

~~45~~47. Di Dato, V., R. Barbarinaldi, A. Amato, F. Di Costanzo, C. Fontanarosa, A. Perna, A. Amoresano, F. Esposito, A. Cutignano, A. Ianora, and G. Romano, Variation in prostaglandin metabolism during growth of the diatom Thalassiosira rotula. *Scientific Reports* **2020**, *10* (1), 5374. 10.1038/s41598-020-61967-3.

~~46~~48. Meyer, N., J. Rettner, M. Werner, O. Werz, and G. Pohnert, Algal Oxylipins Mediate the Resistance of Diatoms against Algicidal Bacteria. *Marine drugs* **2018**, *16* (12), 486. 10.3390/md16120486.

~~47~~49. Russo, E., G. d'Ippolito, A. Fontana, D. Sarno, D. D'Alelio, G. Busseni, A. Ianora, E. von Elert, and Y. Carotenuto, Density-dependent oxylipin production in natural diatom communities: possible implications for plankton dynamics. *The ISME Journal* **2020**, *14* (1), 164-177. 10.1038/s41396-019-0518-5.

~~48~~50. He, Q., H. Yang, L. Wu, and C. Hu, Effect of light intensity on physiological changes, carbon allocation and neutral lipid accumulation in oleaginous microalgae. *Bioresour Technol* **2015**, *191*, 219-228.

~~49~~51. Zhang, Y.-M., H. Chen, C.-L. He, and Q. Wang, Nitrogen Starvation Induced Oxidative Stress in an Oil-Producing Green Alga Chlorella sorokiniana C3. *PLOS ONE* **2013**, *8* (7), e69225. 10.1371/journal.pone.0069225.

~~50~~52. Yilancioglu, K., M. Cokol, I. Pastirmaci, B. Erman, and S. Cetiner, Oxidative Stress Is a Mediator for Increased Lipid Accumulation in a Newly Isolated Dunaliella salina Strain. *PLOS ONE* **2014**, *9* (3), e91957. 10.1371/journal.pone.0091957.

~~51~~53. Renaud, S.M., L.-V. Thinh, G. Lambrinidis, and D.L. Parry, Effect of temperature on growth, chemical composition and fatty acid composition of tropical Australian microalgae grown in batch cultures. *Aquaculture* **2002**, *211* (1), 195-214. 10.1016/S0044-8486(01)00875-4.

~~52~~54. Church, J., J.H. Hwang, K.T. Kim, R. McLean, Y.K. Oh, B. Nam, J.C. Joo, and W.H. Lee, Effect of salt type and concentration on the growth and lipid content of Chlorella vulgaris in synthetic saline wastewater for biofuel production. *Bioresour Technol* **2017**, *243*, 147-153. 10.1016/j.biortech.2017.06.081.

~~53~~55. Watrous, J.D., T.J. Niiranen, K.A. Lagerborg, M. Henglin, Y.-J. Xu, J. Rong, S. Sharma, R.S. Vasan, M.G. Larson, A. Armando, S. Mora, O. Quehenberger, E.A. Dennis, S. Cheng, and M. Jain, Directed Non-targeted Mass Spectrometry and Chemical Networking for Discovery of Eicosanoids and Related Oxylipins. *Cell Chemical Biology* **2019**, *26* (3), 433-442.e4. 10.1016/j.chembiol.2018.11.015.

~~54~~56. Martínez, E., R.K. Cosnahan, M. Wu, S.K. Gadila, E.B. Quick, J.A. Mobley, and J. Campos-Gómez, Oxylipins mediate cell-to-cell communication in Pseudomonas aeruginosa. *Communications Biology* **2019**, *2* (1), 66. 10.1038/s42003-019-0310-0.

~~55~~57. Wang, W., H. Yang, D. Johnson, C. Gensler, E. Decker, and G. Zhang, Chemistry and biology of ω-3 PUFA peroxidation-derived compounds. *Prostaglandins & Other Lipid Mediators* **2017**, *132*, 84-91. 10.1016/j.prostaglandins.2016.12.004.

~~56~~58. Minghetti, L., R. Salvi, M. Lavinia Salvatori, M. Antonietta Ajmone-Cat, C. De Nuccio, S. Visentin, V. Bultel-Poncé, C. Oger, A. Guy, J.-M. Galano, A. Greco, A. Bernardo, and T. Durand, Nonenzymatic oxygenated metabolites of α-linolenic acid B1- and L1-phytoprostanes protect immature neurons from oxidant injury and promote differentiation of oligodendrocyte progenitors through PPAR-γ activation. *Free Radic Biol Med* **2014**, *73*, 41-50. 10.1016/j.freeradbiomed.2014.04.025.

~~57~~59. Lee, Y.Y., J.-M. Galano, H.H. Leung, L. Balas, C. Oger, T. Durand, and J.C.-Y. Lee, Nonenzymatic oxygenated metabolite of docosahexaenoic acid, 4(RS)-4-F4t-neuroprostane, acts as a bioactive lipid molecule in neuronal cells. *FEBS Letters* **2020**, *594* (11), 1797-1808. 10.1002/1873-3468.13774.

~~58~~60. Song, W.L., G. Paschos, S. Fries, M.P. Reilly, Y. Yu, J. Rokach, C.T. Chang, P. Patel, J.A. Lawson, and G.A. Fitzgerald, Novel eicosapentaenoic acid-derived F3-isoprostanes as biomarkers of lipid peroxidation. *The Journal of biological chemistry* **2009**, *284* (35), 23636-43. 10.1074/jbc.M109.024075.

~~59~~61. Praticò, D., F. Smyth Em Fau - Violi, G.A. Violi F Fau - FitzGerald, and G.A. FitzGerald, Local amplification of platelet function by 8-Epi prostaglandin F2alpha is not mediated by thromboxane receptor isoforms. *J Bio Chem* **1996**, *271* (25), 14916-24. 10.1074/jbc.271.25.14916

~~60~~62. Roy, J., C. Oger, J. Thireau, J. Roussel, O. Mercier-Touzet, D. Faure, E. Pinot, C. Farah, D.F. Taber, J.-P. Cristol, J.C.Y. Lee, A. Lacampagne, J.-M. Galano, T. Durand, and J.-Y. Le Guennec, Nonenzymatic lipid mediators, neuroprostanes, exert the antiarrhythmic properties of docosahexaenoic acid. *Free Radical Biology and Medicine* **2015**, *86*, 269-278. 10.1016/j.freeradbiomed.2015.04.014.

~~61~~63. Roy, J., J. Fauconnier, C. Oger, C. Farah, C. Angebault-Prouteau, J. Thireau, P. Bideaux, V. Scheuermann, V. Bultel-Poncé, M. Demion, J.M. Galano, T. Durand, J.C. Lee, and J.Y. Le Guennec, Non-

enzymatic oxidized metabolite of DHA, 4(RS)-4-F(4t)-neuroprostane protects the heart against reperfusion injury. *Free Radic Biol Med* **2017**, *102*, 229-239. 10.1016/j.freeradbiomed.2016.12.005.

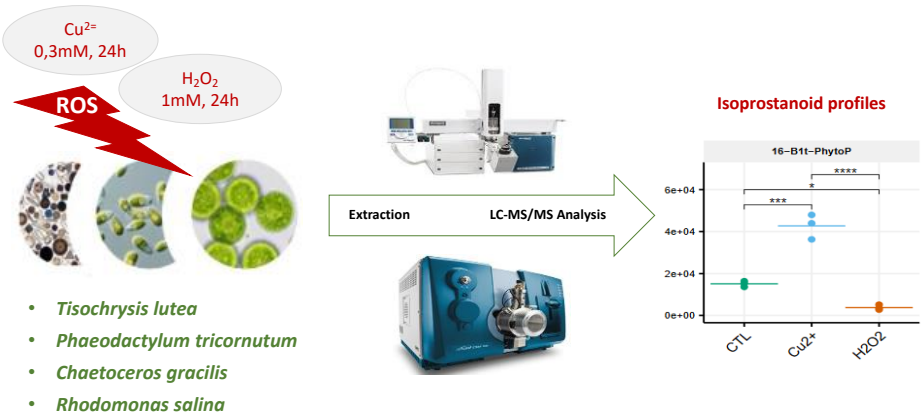

Graphical abstract

Highlights

- Isoprostanoids are the products of non-enzymatic oxidation of polyunsaturated fatty acids (NEO-PUFAs).
- Isoprostanoid analysis in four microalgae was conducted using a liquid mass chromatography tandem mass method.
- Exposure to heavy metal (copper), strongly altered production of NEO-PUFAs in the haptophyte *Tisochrysis lutea* and the diatom *Phaeodactylum tricornutum*
- After hydrogen peroxide stress, changes in isoprostanoid content were observed in the cryptophyte *Rhodomonas salina* and *Phaeodactylum tricornutum*.